Degradation of Paclitaxel and Related Compounds in Aqueous Solutions I: Epimerization

JIAHER TIAN,[1,2] VALENTINO J. STELLA[1]

[1]Department of Pharmaceutical Chemistry, The University of Kansas, Lawrence, Kansas 66047

[2]Wyeth Research, Pearl River, New York 10965

Received 22 November 2006; revised 3 April 2007; accepted 11 May 2007

Published online in Wiley InterScience (www.interscience.wiley.com). DOI 10.1002/jps.21112

ABSTRACT: Paclitaxel and other taxanes have complex structures including the presence of numerous hydrolytically sensitive ester groups and a chiral center that readily undergoes epimerization thus making their kinetics complex. The present study attempts to understand the mechanism of epimerization at the 7-position of paclitaxel, 7-*epi*-taxol, 10-deacetyltaxol, 7-*epi*-10-deacetyltaxol, baccatin III and 10-deacetylbaccatin III. Kinetics were studied as function of temperature, pH and buffer concentration and analyzed using a stability indicating assay and LC/MS to identify degradation products. Epimerization was base catalyzed with no evidence of acid catalysis noted. The observed equilibrium constant for epimerization, K, indicated a thermodynamically more favorable *S*-epimer and a small free energy change between the two epimers. For all of the compounds in this study, removal of the C10 acetyl group increases the epimerization rate in basic aqueous solutions. The observed base-catalyzed epimerization in near neutral to higher pH range suggests a possible rapid deprotonation/protonation of the C7 –OH, followed by a structural rearrangement through a retroaldol/aldol mechanism to form the epimer. Moreover, the rate-limiting step of structure rearrangement most likely occurs with the formation of an enolate intermediate. J Pharm Sci 97:1224–1235, 2008

Keywords: paclitaxel; taxol; 7-epi-taxol; baccatin III; epimerization; degradation; stability

INTRODUCTION

The overall goal of this work was to identify structural elements affecting the rate of epimerization of paclitaxel and some of its analogues in aqueous solution. As a novel anti-tumor drug, paclitaxel has been studied extensively since the late 1970s. Despite many advances only limited information was available on the chemical stability of paclitaxel in aqueous solution. Most early studies were performed in mixed solvents, or in the presence of cyclodextrin.[1–3] The degradation kinetics were mistakenly interpreted as following pseudo-first-order in some instances, while some experimental results indicated that the loss of paclitaxel did not follow first-order kinetics in the basic pH range because of the epimerization competing with the hydrolysis reaction/s.[2,3] The C7 hydroxyl group was one of the most accessible functional groups on the taxane ring structures, and was subject to epimerization. Epimerization of paclitaxel, baccatin III, and various other taxanes during isolation and chemistry studies were noted.[4–11]

This paper focuses on the kinetics of the epimerization of paclitaxel and related compounds in aqueous solution. The reaction kinetics was determined under various pH and temperature conditions in an attempt to clarify the mechanism

Correspondence to: Valentino J. Stella (Telephone: 785-864-3755; Fax: 785-864-5736; E-mail: stella@ku.edu)

Journal of Pharmaceutical Sciences, Vol. 97, 1224–1235 (2008)

of the epimerization which was previously unclear. The influence of the ring structure and substituents was also investigated.

Figure 1 shows the structures of paclitaxel (**1**) and several related compounds also used in this study, including 7-*epi*-taxol (**2**), 10-deacetyltaxol (**3**), 7-*epi*-10-deacetyltaxol (**4**), baccatin III (**5**), and 10-deacetylbaccatin III (**6**). Among these compounds, baccatin III and 10-deacetylbaccatin III represented the diterpene ring structure of paclitaxel and 10-deacetyltaxol, with or without the acetyl group attached to the C10 position, respectively.

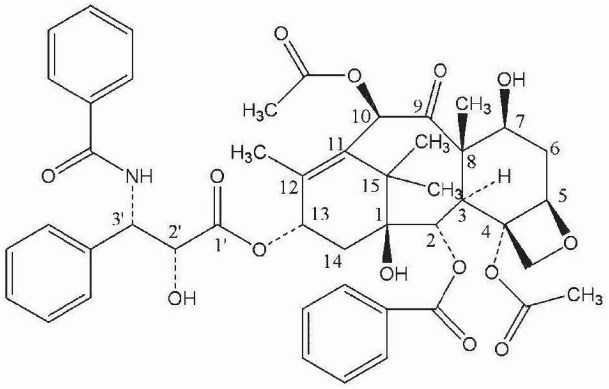

(1) $R_1 = CH_3CO$ $R_2 = OH$ $R_3 = H$
(2) $R_1 = CH_3CO$ $R_2 = H$ $R_3 = OH$
(3) $R_1 = H$ $R_2 = OH$ $R_3 = H$
(4) $R_1 = H$ $R_2 = H$ $R_3 = OH$

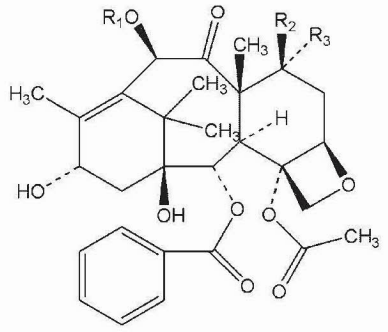

(5) $R_1 = CH_3CO$ $R_2 = OH$ $R_3 = H$
(6) $R_1 = H$ $R_2 = OH$ $R_3 = H$

Figure 1. The structures of paclitaxel and related compounds: paclitaxel (**1**) 7-*epi*-taxol (**2**), 10-deacetyltaxol (**3**), 7-*epi*-10-deacetyltaxol (**4**), baccatin III (**5**), 10-deacetylbaccatin III (**6**).

EXPERIMENTAL

Chemicals and Materials

Paclitaxel, 7-*epi*-taxol, 10-deacetyltaxol, 7-*epi*-10-deacetyltaxol, baccatin III, 10-deacetylbaccatin III were generous gifts from Tapestry Pharmaceuticals (Boulder, CO). Methanol, acetonitrile and other organic solvents were of HPLC grade and were purchased from Fisher Scientific (Fair Lawn, NJ). Hydrochloric acid, formic acid, acetic acid, benzoic acid, sodium hydroxide, sodium acetate, sodium carbonate, sodium bicarbonate, and sodium phosphate salts (monobasic and dibasic) used in preparation of buffer solutions were obtained from Sigma Chemicals Co. (St. Louis, MO). Water used in this study was purified through a Millipore MILLI-QTM system and was glass distilled before use.

pH

The pH of the solution was controlled throughout the reaction by using dilute hydrochloric acid, appropriate buffers, and sodium hydroxide solutions. Reactions at pH 1, 2, and 3 were performed in dilute solutions of hydrochloric acid. Buffer solutions of pH 4 and 5 were prepared from acetic acid and sodium acetate. Buffer solutions of pH 6, 7, and 8 were prepared with sodium phosphate salts (monobasic and dibasic). Buffer solution of pH 9 was prepared with sodium borate and boric acid. Buffer solution of pH 10 was prepared with sodium carbonate and sodium bicarbonate. The kinetic measurements at pH 11 and 12 were performed in dilute sodium hydroxide solutions. As listed in Table 1, the buffer concentration was 1.0 mM except for experiments at pH 1, 2, and 12. The pH values were measured at the beginning and the end of the kinetic experiments. No significant change of pH was observed throughout the reaction. In addition, no buffer catalysis was observed. The pH meter was standardized with appropriate standard buffer solutions of pH 1, 4, 7, and 10 at the temperatures of the kinetic experiments.

HPLC Analytical Assays

To simultaneously detect and quantify the presence of the starting compound, its epimer, and other degradation products, a stability indicating HPLC–UV assay was developed. The HPLC system employed in this study consisted of a Shimadzu

Table 1. The Composition and Measured pH of the Buffer Used in Kinetic Experiments of 10-Deacetylbaccatin III

Buffer Composition	Concentration (mM)	Measured pH
HCl	100.0	1.09
HCl	10.0	1.99
HCl	1.0	3.05
CH_3COOH/CH_3COONa	1.0	4.53
CH_3COOH/CH_3COONa	1.0	5.18
NaH_2PO_4/Na_2HPO_4	1.0	6.74
NaH_2PO_4/Na_2HPO_4	1.0	7.11
NaH_2PO_4/Na_2HPO_4	1.0	7.61
$H3BO_3/Na_2B_4O_7$	1.0	9.04
$NaHCO_3/Na_2CO_3$	1.0	9.81
NaOH	1.0	10.79
NaOH	10.0	11.82

SCL 10A system controller, a Sil-10A auto injector, two LC-10AT pumps, and a SPD-10A UV spectrophotometric detector. The detection wavelength was set at 230 nm for all analytes. The detection signal was directly recorded on to a PC and the chromatograms were reprocessed by the CLASS-VP Chromatography Data System program of Shimadzu. Isocratic elution at ambient temperature was conducted on a Hypersil ODS C-18 column (Alltech) with particle size of 5 μm, and dimensions of 250 mm × 4.6 mm. The mobile phase, acetonitrile–water mixture with 0.1% (v/v) formic acid, was delivered at a flow rate of 1.0 mL/min. The acetonitrile and the aqueous portion were filtered separately and then mixed. The final mixture was degassed by sonication for 30 min prior to using. The percentage of acetonitrile was varied, from 25% to 50%, with different compounds to provide optimum separation. Formic acid was chosen over trifluoroacetic acid, because of its compatibility with mass spectrometry. A 20 μL aliquot of the sample was injected each time through the autosampler. For paclitaxel, 10-deacetyltaxol, 7-*epi*-taxol, 7-*epi*-10-deacetyltaxol, baccatin III, and 10-deacetylbaccatin III, the molar concentrations of individual compound were then calculated based on the measured peak areas and the standard curves of HPLC assays. While some pure compounds were unavailable, they were assumed to have the same molar extinction coefficients for UV absorbance as their corresponding epimers (i.e., 7-*epi*-10-deacetylbaccatin III vs. 10-deacetylbaccatin III), due to the similarity of their chemical structures.

Mass Spectrometry

Identification and profiling of epimerization and degradation products was performed using a Waters Alliance 2690 HPLC system connected to a Micromass Quattro Micro Tandem Quadruple mass spectrometer. The instrument was also equipped with a Waters 2487 Dual Absorbance UV detector. The column used was an AllTech Hypersil C18 column with particle size of 5 μm, and dimensions of 250 mm × 4.6 mm. The mobile phase, acetonitrile–water mixture with 0.1% (v/v) formic acid, was delivered at a flow rate of 1.0 mL/min. The system was operated at an electrospray source block temperature of 120°C, a desolvation temperature of 350°C, a cone voltage of 18 kV. For HPLC–UV–MS mode, the flow rate was 0.833 mL/min versus 0.167 mL/min for UV and MS, respectively. The molecules undergo electron spray ionization in the positive ion mode. The sample injection volume was 40 μL.

With positive ion electrospray (ES+) ionization mode, adduct formation was one of the common complexities in LC–MS. For some molecules being analyzed, adduct ions like $[M + Na]^+$, $[M + K]^+$ or $[M + NH_4]^+$ were abundant in the spectra.

Kinetic Procedures

Stock solutions of 10-deacetylbaccatin III, baccatin III, paclitaxel, 7-*epi*-taxol, 10-deacetyltaxol, and 7-*epi*-10-deacetyltaxol were prepared by accurately weighing sample powder and dissolving them in an appropriate amount of acetonitrile to obtain a concentration of 125 μg/mL. Stock solutions used for kinetic study were made fresh, and were stored at 4°C in a refrigerator shortly before using. From the stock solutions, working standards were prepared by dilution with acetonitrile to various concentrations.

The reaction kinetics for interconversion between epimers was investigated in aqueous solutions at pH 1–12. For the kinetic experiments at 25°C, 24.2 mL of appropriate buffer solutions were equilibrated in a waterbath at 25.0 ± 0.1°C, and the epimerization was initiated by adding 0.8 mL of the stock solution (125 μg/mL in acetonitrile) into the reaction buffer. This resulted in an initial reaction concentration of 2.0 μg/mL. At various time intervals, aliquots (0.8 mL) of the reaction solutions were withdrawn, and analyzed by HPLC. The reactions at basic pH were quenched by adding dilute hydrochloric acid solution to adjust the pH close to 5.

 DOI 10.1002/jps

For the stability studies at elevated temperatures at 37, 50, and 70°C, vials containing sample solutions were placed in thermostatically controlled ovens. The reaction solutions were maintained at the desired temperature throughout the kinetic study. Portions were removed from the reaction solution at appropriate intervals. The samples were quickly cooled in ice water to quench the reaction, and followed immediately by HPLC analysis.

RESULTS AND DISCUSSION

Epimerization of 10-Deacetyl Baccatin III

Order of Reaction and Observed Rate Constants

A typical HPLC chromatogram of the epimerization of 10-deacetyl baccatin III is shown in Figure 2, indicating that the starting compound *S*-epimer, and the epimerization and degradation products can be separated. The formation of one initial product, with a longer retention time than 10-deacetylbaccatin III, was observed. Using LC–MS–MS, the initial product was identified as the 7-epimer of 10-deacetyl baccatin III since it had the same molecular weight. With more reaction time, both epimers further degraded into fragmented products.

Figure 3 shows typical plots of the percent residual *R*- and *S*-epimers of the initial concentration of 10-deactyl baccatin III (*S*-epimer), throughout the reaction at pH 10.8 and 50°C. The time course indicated that 10-deacetylbaccatin III and its epimer reached a relatively fast pseudo-equilibrium and was followed by further degradation. Obviously, neither the loss of the starting compound nor the formation of products should follow simple first-order kinetics.

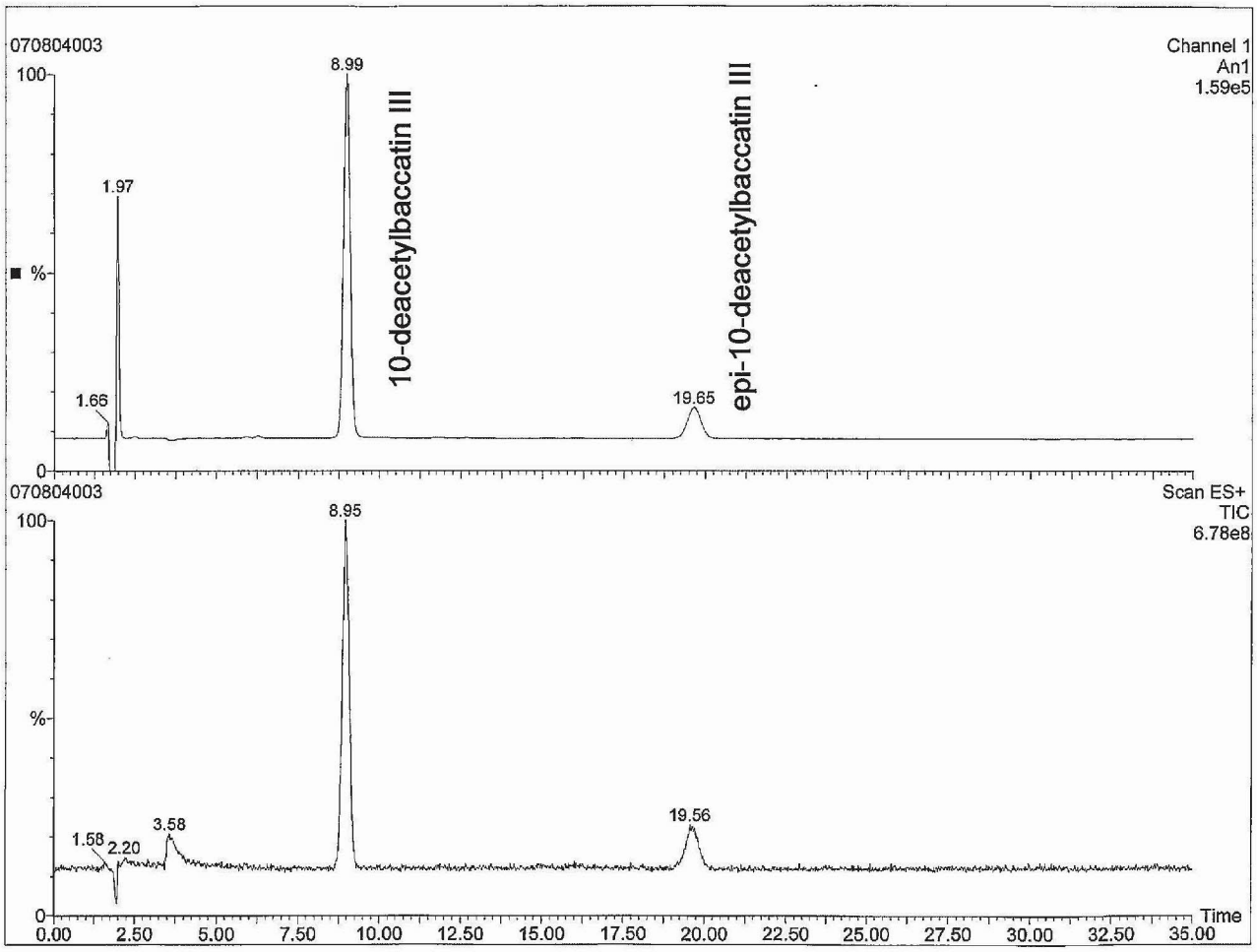

Figure 2. HPLC chromatogram and MS-data for the degradation of 10-deacetyl baccatin III and formation of its epimer as the initial primary product in aqueous solution at pH 10.8, 25°C, and 5 min reaction time.

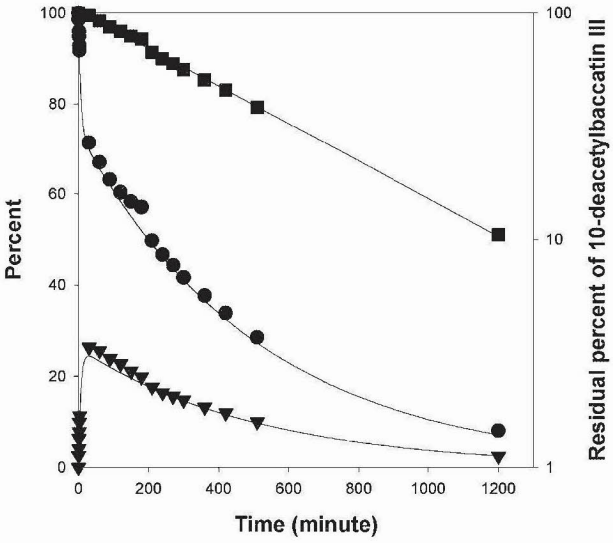

Figure 3. Time courses for the loss of *S*-epimer (●), formation and loss of *R*-epimer (▼), and total 10-deacetylbaccatin III disappearance (■, total residual of the *S*- and *R*-epimers) at pH 10.8 and 25°C. The total residual of 10-deacetylbaccatin III is plotted semilogarithmically versus time. The solid lines represent the best fit to Eqs. (9)–(11).

rate constants of 10-deacetylbaccatin III and its epimer, due to hydrolysis of ester groups. This scheme can be described by Eqs. (1) and (2)

$$\frac{d[S]}{dt} = -k_1[S] + k_2[R] - k_3[S] \quad (1)$$

$$\frac{d[R]}{dt} = k_1[S] - k_2[R] - k_4[R] \quad (2)$$

Solving these differential equations leads to Eqs. (3)–(8)

$$[S] = c_1 k_2 e^{\lambda_1 t} + c_2 k_2 e^{\lambda_2 t} \quad (3)$$

$$[R] = c_1(\lambda_1 + k_1 + k_3) e^{\lambda_1 t} + c_2(\lambda_2 + k_1 + k_3) k_2 e^{\lambda_2 t} \quad (4)$$

where

$$c_1 = \frac{S_0(\lambda_2 + k_1 + k_3) - R_0 k_2}{k_2(\lambda_2 - \lambda_1)} \quad (5)$$

$$c_2 = \frac{-S_0(\lambda_1 + k_1 + k_3) + R_0 k_2}{k_2(\lambda_2 - \lambda_1)} \quad (6)$$

and

$$\lambda_1 = \frac{-(k_1 + k_2 + k_3 + k_4) + \sqrt{(k_1 + k_3 - k_2 - k_4)^2 + 4k_1k_2}}{2} \quad (7)$$

$$\lambda_2 = \frac{-(k_1 + k_2 + k_3 + k_4) - \sqrt{(k_1 + k_3 - k_2 - k_4)^2 + 4k_1k_2}}{2} \quad (8)$$

The semilogarithmic plot of the percent residual total 10-deacetylbaccatin III (sum of both epimers) versus time was linear which indicated that the overall secondary degradation pathway followed pseudo-first-order kinetics. The disappearance of the *S*-epimer and the appearance of the *R*-epimer were also measured at various pH values (1–12) and temperatures. The epimerization, as expected, was found to be reversible in neutral and basic pH range, while no significant epimerization was observed under acidic pH conditions. In addition, the overall secondary degradation, after the relatively fast epimerization, follows pseudo-first-order kinetics at any given constant pH and temperature.

From these results, the concentration-time profiles at various pH values are thought to be a consequence of the reaction scheme illustrated in Figure 4a, where k_1 is the epimerization rate constant from the *S*-epimer to *R*-epimer, k_2 is the reverse reaction, and k_3 and k_4 the degradation

Due to the similarity of the chemical structures of the *R*- and *S*-epimers, it was reasonable to assume that they have identical rate constants for further hydrolytic degradation. A reasonable assumption is to set k_3 equal to k_4. Therefore, the following kinetic equations can be written for the *R*- and *S*-epimers:

$$[S] = \frac{[S]_0 k_2 + [R]_0 k_2}{k_1 + k_2} \exp(-k_3 t) + \frac{[S]_0 k_1 - [R]_0 k_2}{k_1 + k_2} \exp[-(k_1 + k_2 + k_3)t] \quad (9)$$

$$[R] = \frac{[S]_0 k_1 + [R]_0 k_1}{k_1 + k_2} \exp(-k_3 t) + \frac{[S]_0 k_1 - [R]_0 k_2}{k_1 + k_2} \exp[-(k_1 + k_2 + k_3)t] \quad (10)$$

$$[R] + [S] = \{[R]_0 + [S]_0\} \exp(-k_3 t) \quad (11)$$

DOI 10.1002/jps

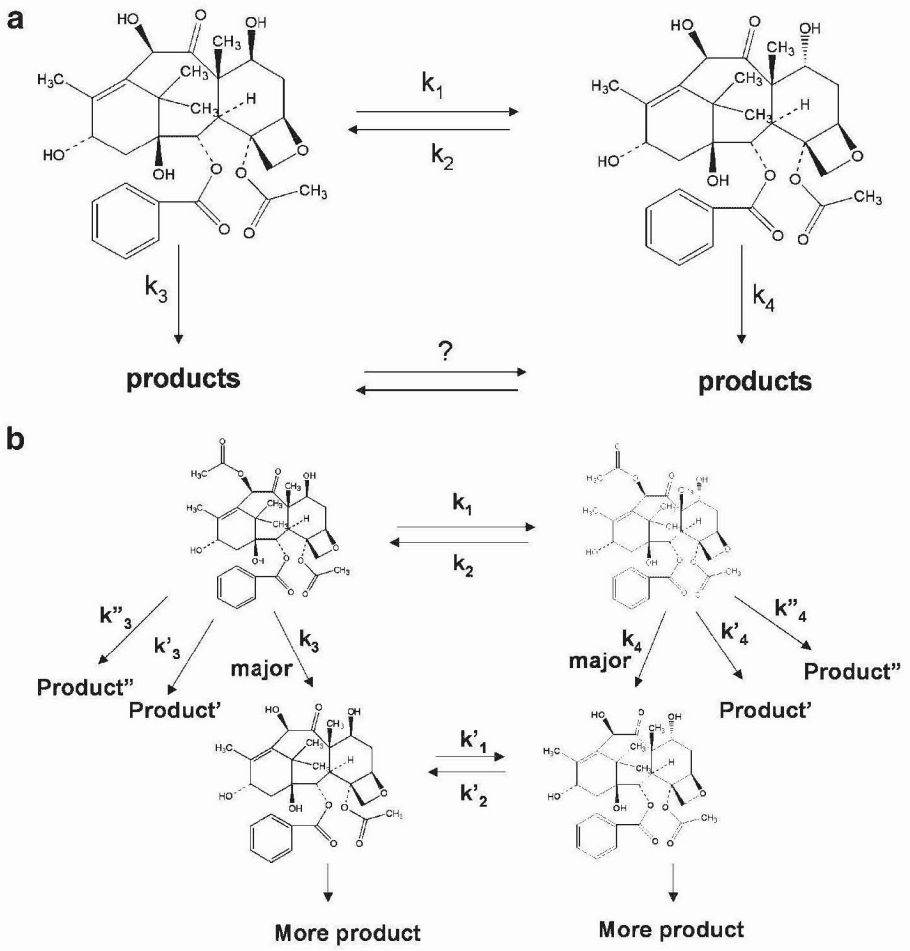

Figure 4. The proposed pathways for the epimerization of 10-deacetylbaccatin III (a), baccatin III (b), and secondary degradation under basic pH.

This assumption was supported by the linear plots of the total degradation profile on semilogarithmic scale shown in Figure 3. The semilogarithmic plots should curve at the early stage of the decomposition if either the *R*- or *S*-epimer decomposes faster than the other, unless k_1 and k_2 are overwhelmingly larger than k_3.

Epimerization of Baccatin III

The degradation of baccatin III in neutral to basic pH range seemed to be more complex than that of 10-deacetylbaccatin III. Figure 5 shows typical plots of the percent residual *R*- and *S*-epimers of baccatin III (*S*-epimer), at pH 10.8 and 25.0°C. The time course indicates an initial epimerization reaction to generate the *R*-epimer, followed by further degradation, leading to multiple products. The ester groups at C2, C4, and C10 positions might be expected to undergo hydrolysis simultaneously, and the overall degradation rate constant is the sum of the individual hydrolytic rate constants of all three ester bonds. A proposed reaction scheme is illustrated in Figure 4b.

Effect of pH on Epimerization

The first-order rate constants of reversible epimerization, k_1 and k_2, for 10-deaceylbaccatin III and baccatin III under various temperature and pH conditions are given in Tables 2 and 3. The individual rate constant values were obtained from the best multi-variance regression of experimental data to Eqs. (9)–(11), using SigmaPlot program (v 7.101, SPSS, Inc., Chicago, IL). The value of k_3 was obtained from the pseudo first-order kinetics of the total loss of the drug (sum of *R*- and S-epimers). The data for the loss of the

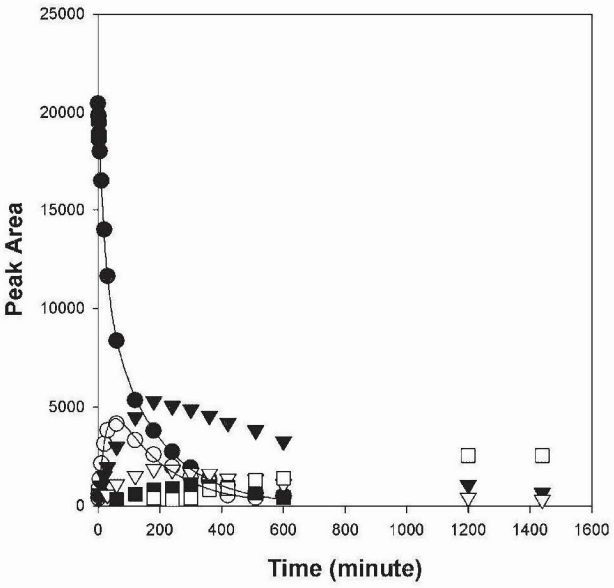

Figure 5. Time course of the degradation of baccatin III in aqueous solution at pH 10.77, $T = 25°C$. Symbol key: baccatin III (●); baccatin V (7-*epi*-baccatin III, ○); 10-deacetylbaccatin III (▼); 7-*epi*-10-deacetylbaccatin III (▽); unidentified product 1 (■); unidentified product 2 (□). The solid lines represent the best fit to the Eqs. (9) and (10), according to the measured loss of baccatin III (●), formation and loss of baccatin V (7-*epi*-baccatin III, ○).

starting *S*-epimer and the formation of the *R*-epimer are fitted into Eqs. (9) and (10) to generate k_1 and k_2 values. Both forward and reverse rates of epimerization increased rapidly with increasing pH consistent with an apparent base-catalyzed reaction.

The equilibrium constant for epimerization, *K*, was also calculated from the ratio k_1/k_2. Since both 10-deacetylbaccatin III and baccatin III are neutral molecules, *K* values should be independent of pH. This was seen at pH values higher than 9, while the values determined in the lower pH range might bear more experimental error due to the slow reactions. The *S*-epimer is the thermodynamically more stable isomer.

Effect of Temperature on Epimerization

The epimerization of 10-deacetylbaccatin III was studied at pH 7.61 and 25, 50, and 70°C. The values of rate constants are given in Table 4. As expected, both forward and reverse rate constants were increased rapidly with increasing temperature. The *S*-epimer is more stable at all temperatures, while the forward rate constant k_1 (*S*- to *R*-epimer) increased slightly faster than k_2, with increasing temperature.

When this data was fit to the Eyring equation,[12] the plot, although linear, did suggest some curvature. Estimated values of the activation enthalpy, $\Delta H^{\neq}$, and activation entropy, $\Delta S^{\neq}$, are listed in Table 5.

pH-Rate Profiles for the Epimerization of 10-Deacetylbaccatin III and Baccatin III

The pH dependence of the first-order epimerization rate constants, k_1 and k_2, of 10-deacetylbaccatin III and baccatin III at 25.0°C, are shown in Figures 6 and 7, respectively. In both figures, the observed rate constants for the epimerization increased rapidly and uniformly with increasing pH. The slopes of these straight-line portions of log k versus pH profiles are close to unity, thus, it is likely that the reversible epimerization is base-catalyzed.

In near neutral and basic pH range, base-catalyzed epimerization seems predominant compared to any water catalysis. In this pH range no significant buffer catalysis was observed. Therefore, these pH rate profiles can be described by Eq. (12):

$$k_{pH} = k_B\left(\frac{K_w}{\alpha_H}\right) \tag{12}$$

where K_w is the dissociation constant for water and α_H is the activity of hydrogen ions as measured by a glass electrode.

Table 2. First-Order Rate Constants, k_1 and k_2, and Equilibrium Constant *K* of Epimerization of 10-Deacetylbaccatin III at Various pH in Aqueous Solution at 25°C, as Defined in Figure 4

	pH				
	7.11	7.61	9.04	10.79	11.82
k_1 (h^{-1})	$6.4 \pm 1.0 \times 10^{-4}$	$2.5 \pm 0.2 \times 10^{-3}$	$4.6 \pm 0.1 \times 10^{-2}$	2.29 ± 0.36	33.5 ± 1.3
k_2 (h^{-1})	$5.4 \pm 6.6 \times 10^{-3}$	$9.4 \pm 3.5 \times 10^{-3}$	0.118 ± 0.005	6.44 ± 1.09	83.4 ± 3.1
K (k_1/k_2)	0.12	0.27	0.39	0.36	0.40

 DOI 10.1002/jps

Table 3. First-Order Rate Constants, k_1 and k_2, and Equilibrium Constant K of Epimerization of Baccatin III at Various pH in Aqueous Solution at 25°C, as Defined in Figure 4

	pH				
	7.07	7.68	9.81	10.77	11.93
k_1 (h^{-1})	$4.8 \pm 12 \times 10^{-4}$	$2.7 \pm 4.0 \times 10^{-3}$	$5.9 \pm 0.4 \times 10^{-2}$	0.92 ± 0.07	8.77 ± 1.44
k_2 (h^{-1})	$1.0 \pm 9.7 \times 10^{-2}$	$1.2 \pm 5.0 \times 10^{-2}$	$8.7 \pm 1.2 \times 10^{-2}$	1.34 ± 0.21	12.8 ± 3.22
K (k_1/k_2)	0.048	0.22	0.69	0.68	0.65

Table 4. First-Order Rate Constants, k_1 and k_2, and Equilibrium Constant K of Epimerization of 10-Deacetylbaccatin III in Aqueous Solution at pH 7.61 and Various Temperatures

	Temperature (°C)		
	25	50	70
k_1 (h^{-1})	$2.5 \pm 0.2 \times 10^{-3}$	0.159 ± 0.035	0.564 ± 0.162
k_2 (h^{-1})	$9.4 \pm 3.5 \times 10^{-3}$	0.358 ± 0.099	0.978 ± 0.586
K (k_1/k_2)	0.27	0.44	0.58

Table 5. Temperature Dependence of Epimerization of 10-Deacetylbaccatin III Measured at pH 7.61

	$\Delta H^{\neq}$ (kcal mol^{-1})	$\Delta S^{\neq}$ (e.u.)	$\Delta G^{\neq}$ (kcal mol^{-1})
k_1 of epimerization	24.4 ± 4.8	-4.5 ± 0.9	25.8 ± 5.1
k_2 of epimerization	20.8 ± 4.5	-13.7 ± 3.2	24.9 ± 5.4

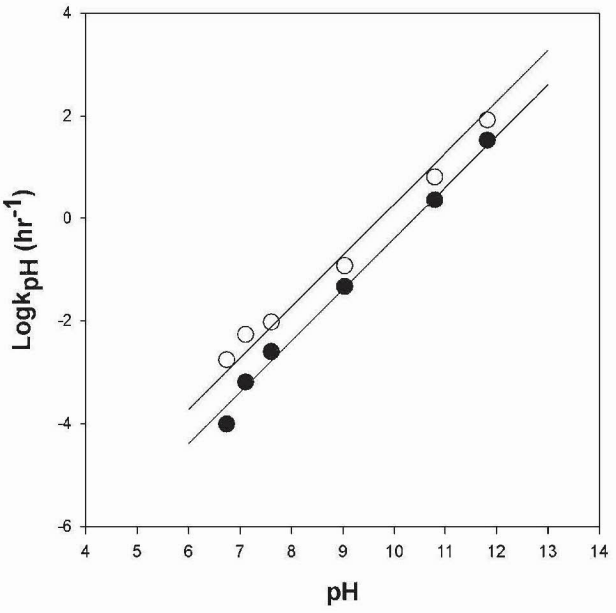

Figure 6. pH-rate profile for the values k_1 (●) and k_2 (○) used to describe the epimerization of 10-deacetylbaccatin III at various pH values, 25°C. The solid line represents the best fit to Eq. (12) where $k_{1B} = 4.92 \pm 0.82 \times 10^3$ M^{-1} h^{-1}; $k_{2B} = 1.24 \pm 0.13 \times 10^4$ M^{-1} h^{-1}.

In Figures 6 and 7, the solid lines represent the theoretical curves calculated by Eq. (12). The values for the second-order rate constants obtained from the fit are reported in Table 6. The results show that the second-order base-catalyzed rate constants for the epimerization of 10-deacetylbacatin III, both forward and reverse, are faster compared to that of baccatin III.

Epimerization of Paclitaxel and Other Compounds

Figures 8–11 show the epimerization of paclitaxel, 7-*epi*-taxol, 10-deacetyltaxol, 7-*epi*-10-deacetyltaxol at pH 7.72 and 70°C. At this elevated temperature, the solubility of these compounds was sufficient for quantitative analysis. The semilogarithmic plot of the total loss of the starting compound (sum of both epimers) versus time was reasonably linear which indicated that the overall secondary degradation followed pseudo-first-order kinetics disregarding the epimerization. The experimental data yielded good fits for Eqs. (9) and (10). The obtained first-order rate constants for reversible epimerization, k_1

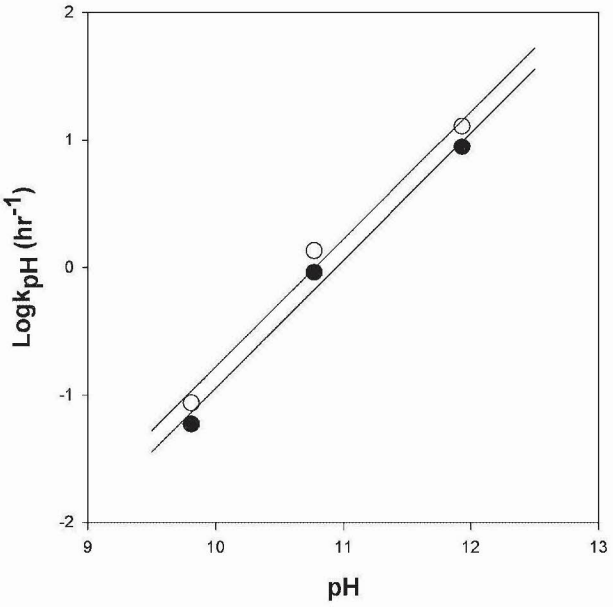

Figure 7. pH-rate profile for the values k_1 (●) and k_2 (○) used to describe the epimerization of baccatin III at various pH values, 25°C. The solid line represents the best fit to Eq. (12) where $k_{1B} = 1.05 \pm 0.34 \times 10^3$ M^{-1} h^{-1}; $k_{2B} = 1.52 \pm 0.41 \times 10^3$ M^{-1} h^{-1}.

(*S*- to *R*-epimer) and k_2 (*R*- to *S*-epimer), for paclitaxel and its analogues at pH 7.7 and 70°C are given in Table 7. The rate constants obtained from the epimerization of the *S*- and *R*-epimers, starting from either epimer, are virtually the same. The *S*-epimer was the thermodynamically more stable specie for all of the compounds at this condition. The results suggest that paclitaxel and its derivatives follow the similar reaction mechanism for 10-deacetylbaccatin III and baccatin III, described previously in Figure 4.

Influence of the Substituents on Epimerization

By comparing the epimerization data for paclitaxel and its analogues, which have the same fundamental diterpene ring skeleton but different substituents at the C10 and C13 position, the substituent effect on the epimerization rate constants can be seen. As listed in Tables 2, 3 and 6, 10-deacetylbaccatin III exhibits faster base-catalyzed epimerization rates than baccatin III, at

Table 6. The Second-Order Rate Constants for Epimerization of 10-Deacetylbaccatin III and Baccatin III at 25°C under Basic pH Conditions

	k_{1B} (M^{-1} h^{-1})	k_{2B} (M^{-1} h^{-1})
10-Deacetylbaccatin III	$4.92 \pm 0.82 \times 10^3$	$1.24 \pm 0.13 \times 10^4$
Baccatin III	$1.05 \pm 0.34 \times 10^3$	$1.52 \pm 0.41 \times 10^3$

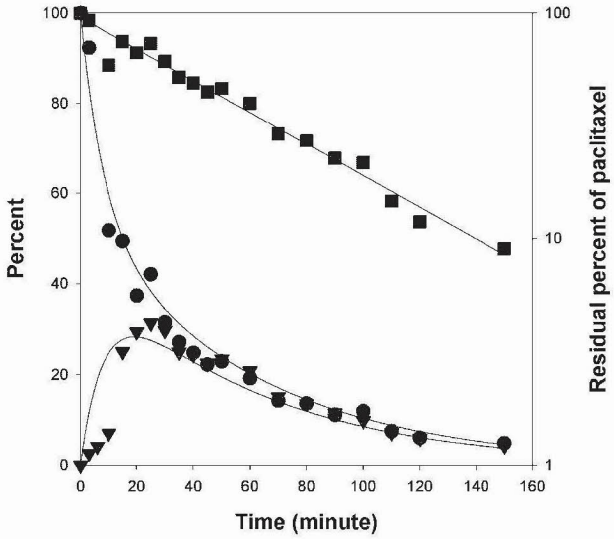

Figure 8. Time courses for the loss of *S*-epimer (●), formation and loss of *R*-epimer (▼), and total paclitaxel disappearance (■, total of the *S*- and *R*-epimers) at pH 7.72 and 70°C. The total paclitaxel is plotted semi-logarithmically versus time. The solid lines represent the best fit to Eqs. (9)–(11).

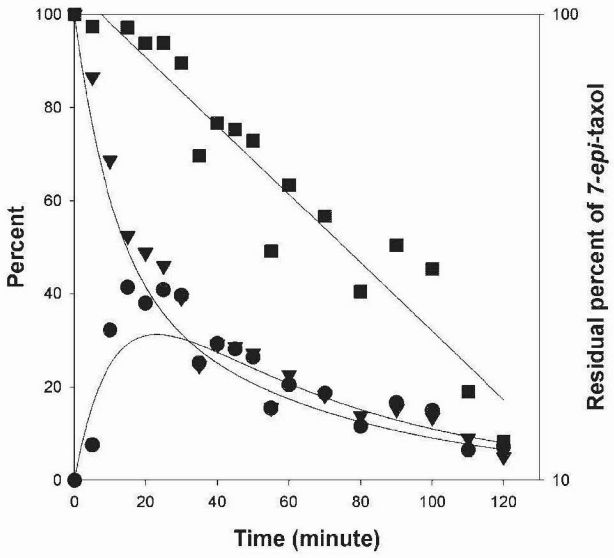

Figure 9. Time courses for the loss of *S*-epimer (▼), formation and loss of *R*-epimer (●), and total 7-*epi*-taxol disappearance (■, total of the *S*- and *R*-epimers) at pH 7.72 and 70°C. The total 7-*epi*-taxol is plotted semilogarithmically versus time. The solid lines represent the best fit to Eqs. (9)–(11).

DOI 10.1002/jps

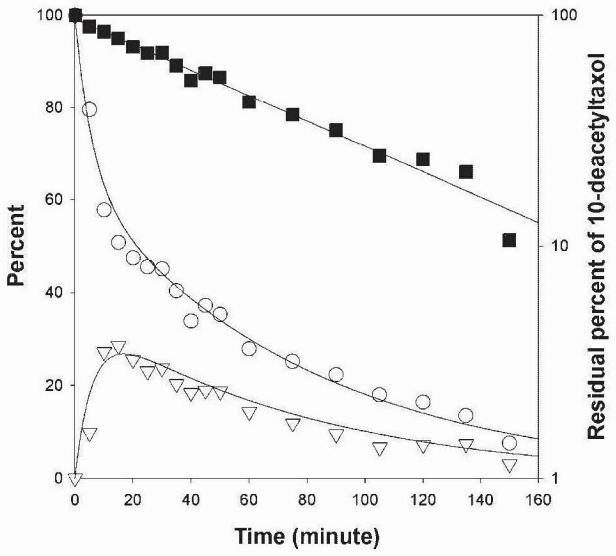

Figure 10. Time courses for the loss of *S*-epimer (○), formation and loss of *R*-epimer (▽), and total 10-deacetyltaxol disappearance (■, total of the *S*- and *R*-epimers) at pH 7.72 and 70°C. The total 10-deacetyltaxol is plotted semilogarithmically versus time. The solid lines represent the best fit to Eqs. (9)–(11).

25°C. In addition, 10-deacetyltaxol and its epimer show faster epimerization rates than paclitaxel and epitaxol, at 70°C. This is compatible with the results for 10-deacetylbaccatin III and baccatin III, although to a smaller extent. Therefore,

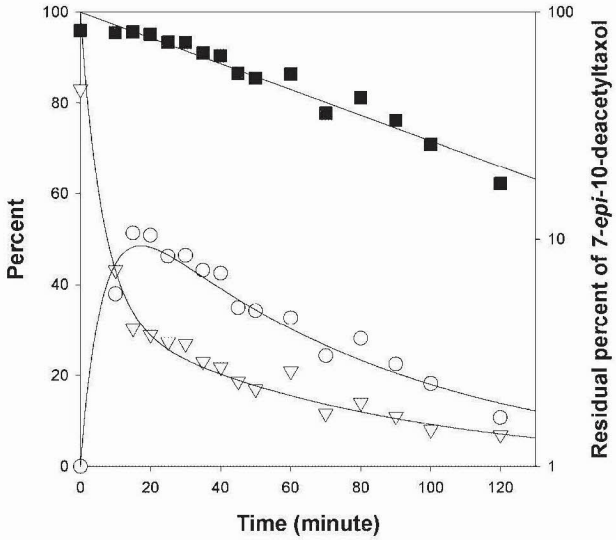

Figure 11. Time courses for the loss of *S*-epimer (▽), formation and loss of *R*-epimer (○), and total 7-*epi*-10-deacetyltaxol disappearance (■, total of the *S*- and *R*-epimers) at pH 7.72 and 70°C. The total 7-*epi*-10-deacetyltaxol is plotted semilogarithmically versus time. The solid lines represent the best fit to Eqs. (9)–(11).

Table 7. First-Order Rate Constants, k_1 and k_2, and Equilibrium Constant K of Epimerization of Paclitaxel and Related Compounds at pH 7.72, 70°C, According to Figure 4

Starting Compound	k_1 (h^{-1})	k_2 (h^{-1})	K (k_1/k_2)
Paclitaxel	2.81 ± 1.01	3.42 ± 2.82	0.822
7-*epi*-taxol	2.03 ± 1.38	2.48 ± 0.56	0.821
10-Deacetyltaxol	3.31 ± 0.66	5.93 ± 1.51	0.558
7-*epi*-10-deacetyltaxol	2.96 ± 1.44	5.78 ± 1.92	0.512

removal of the C10 acetyl group increases the epimerization rate in aqueous solution.

Both 10-deacetylbaccatin III and 10-deacetyltaxol have the identical taxane ring structure, the latter has an additional side chain attached to the C13 position. As seen by comparing the rate constants in Tables 4 and 7, 10-deacetyltaxol shows faster epimerization rates than 10-deacetylbaccatin III at 70°C after the influence from the small pH variance is corrected. This difference could possibly be due to the conformational change of the taxane ring, caused by the side chain through hydrophobic interaction between the C4 acetyl group and the two phenyl groups. This additional interaction might distort the taxane ring and cause a slightly higher strain, therefore increase the free energy level of the ground states of both epimers, which then leads to faster epimerization in both directions.

Finally, the *S*-epimer is found to be more favorable than the *R*-epimer, for all of the compounds in this study, with or without the 10-acetyl and side chain groups. This observation was not in total agreement with some previously published information.[10,13] The 7-epitaxol and other α-epimers (*R*-epimer) were determined as the more stable form in alcohol and other mixed solvents. This observation was thought to be due to the strong hydrogen bonding formed between the 7α-hydroxyl to the acyl oxygen of the 4α-acetate, first observed in baccatin III crystal structure.[11] However, NMR studies of paclitaxel and other taxanes in solution indicated that some original intramolecular hydrogen bonding could be lost with the concomitant appearance of the new hydrophobic interactions.[14,15] For paclitaxel and its derivatives investigated in this study, their equilibrium constant for epimerization, K, does not show big variance from a range of 0.2 to 1 under most experimental conditions. That observation indicates a small free energy change between the two epimers. For example, a typical

K value of 0.3 (or 3), is translated to a free energy change of approximately 0.5 kcal mol^{-1}. Moreover, others suggest that solvent polarity exhibits a strong effect on the conformation of taxanes in solution.[16] Such a conformation change (i.e., from methanol to aqueous solution) should lead to an energy change enough to cause the shift of equilibrium. Therefore, it is quite reasonable to expect paclitaxel and its analogues to show various ratios of epimers in aqueous solution, organic solvent, and mixed solvents.

Mechanism of Base-Catalyzed Epimerization

A "Retroaldol/aldol intramolecular mechanism" was proposed by McLaughlin et al.,[6] as the mechanism of epimerization for paclitaxel (Scheme 1). In this proposed mechanism, the hydroxyl hydrogen is transferred from C7 to the C9 carbonyl with concomitant aldehyde formation at C7, ring cleavage between C7 and C8, doublebond formation between C8 and C9, and hence enol formation at C9 in a concerted mechanism. Free rotation of the single bond between C6 and C7 allows the electron density in the C8–C9 alkene to attack the aldehyde carbonyl from either face of the C7 carbon, forming either paclitaxel or 7-*epi*-paclitaxel.

This mechanism should show minimal pH dependence since it is an intramolecular reaction in a relatively "closed system". However, a strong pH dependence has been observed for both 10-deacetylbaccatin III and baccatin III epimerization in this study. This indicated that the epimerization more likely occurs with forming an enolate intermediate shown in Scheme 2. This mechanism can be written in terms of the fast abstraction of the proton of the 7-hydroxyl group by an external base. The deprotonated specie then undergoes structural rearrangement in the rate-determining step in which the single bond between C7 and C8 is cleaved and the enolate on C9 is formed simultaneously, as described in Scheme 2. The reaction is reversible via the same intermediate. This proposed mechanism is compatible to the observed base-catalyzed epimerization in high pH range and the lack of buffer concentration dependency. It would still be considered a retroaldol/aldol reaction.

This proposed mechanism implies that a substituent with stronger electron withdrawing effect might stabilize the deprotonated specie making the C7–C8 bond easier to cleave, thus, increasing the epimerization rate. However, under basic pH condition, 10-deacetyl baccatin III exhibits forward and reverse epimerization rate constants faster than those of baccatin III (shown in Tabs. 2 and 3) even though the latter has more electron-withdrawing influence from the C10 acetyl group. A possible explanation is that the 10-hydroxyl group effectively stabilized the enolate intermediate by forming a hydrogen bond during the reaction, which is impossible for baccatin III (see Scheme 3). A similar comparison can be made between paclitaxel and 10-deacetyltaxol (shown in Tab. 7), although to a smaller extent.

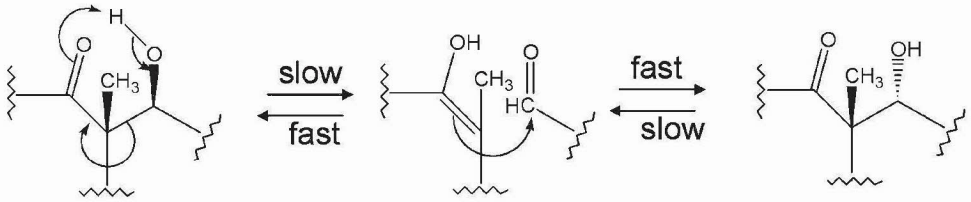

Scheme 1. Mechanism of epimerization proposed by McLaughlin et al.[6]

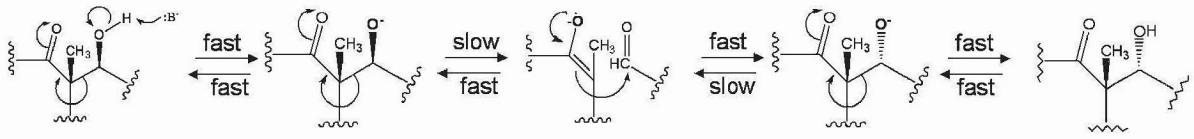

Scheme 2. Proposed mechanism for base-catalyzed epimerization.

 DOI 10.1002/jps

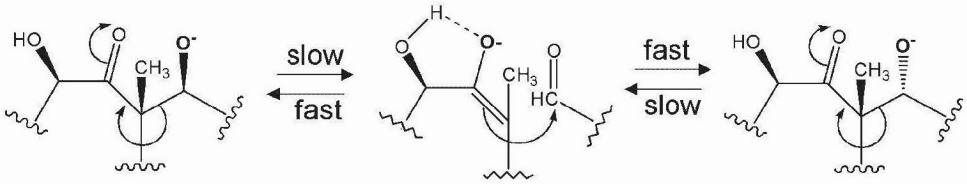

Scheme 3. Proposed mechanism for epimerization of 10-deacetylbaccatin III.

CONCLUSIONS

Paclitaxel and some related taxanes, including 7-*epi*-taxol, 7-*epi*-taxol, 10-deacetyltaxol, 7-*epi*-10-deacetyltaxol, baccatin III, and 10-deacetylbaccatin III, epimerize reversibly under basic and neutral pH conditions in aqueous solution. Both *S*- and *R*-epimers further hydrolyze, while no other reaction such as dehydration of hydroxyl group or hydrolytic opening of the oxetane ring was observed under base conditions. Removal of the C10 acetyl group increases the epimerization rate in basic aqueous solutions. The observed base-catalyzed epimerization in near neutral to higher pH range suggests a possible rapid deprotonation/protonation of the C7 –OH, followed by a structural rearrangement through a retroaldol/aldol mechanism to form the epimer. The rate-limiting step of structure rearrangement most likely occurs with the formation of an enolate intermediate. No significant epimerization was observed under acidic pH conditions.

ACKNOWLEDGMENTS

The authors greatly appreciate the contribution and support by Dr. Richard Schowen. The authors also gratefully acknowledge the support of Dr. Gunda George and Tapestry Pharmaceuticals, Inc. as suppliers of paclitaxel and other related compounds.

REFERENCES

1. Waugh WN, Trissel LA, Stella VJ. 1991. Stability, compatibility, and plasticizer extraction of taxol (NSC-125973) injection diluted in infusion solutions and stored in various containers. Am J Hosp Pharm 48:1520–1524.
2. MacEachern-Keith GJ, Butterfield LJ, Mattina IMJ. 1997. Paclitaxel stability in solution. Anal Chem 69:72–77.
3. Dordunoo SK, Burt HM. 1996. Solubility and stability of taxol: Effects of buffers and cyclodextrins. Int J Pharm 133:191–201.
4. Kingston DGI. 1991. The chemistry of taxol. Pharmacol Therap 52:1–34.
5. Kingston DGI, Molinero AA, Rimoldi JM. 1993. The taxane diterpenoids. Prog Chem Org Nat Prod 61:206.
6. McLaughlin JL, Miller RW, Powell RG, Smith CR. 1981. 19-Hydroxybaccatin III, 10-deacetylcephalomannine, and 10-deacetyltaxol: New antitumor taxanes from Taxus wallichiana. J Nat Prod 44: 312–319.
7. Miller RW. 1980. A brief survey of Taxus alkaloids and other taxane derivatives. J Nat Prod 43:425–437.
8. Fang W, Fang Q, Liang X. 1997. Reinvestigation to the C-7 epimerization of paclitaxel and related taxoids under basic conditions. Synth Commun 27:2305–2310.
9. Magri NF, Kingston DGI. 1986. Modified taxols. 2. Oxidation products of taxol. J Org Chem 51:797–802.
10. Samaranayake G, Magri NF, Jitrangsri C, Kingston DGI. 1991. Modified taxols. 5. Reaction of taxol with electrophilic reagents and preparation of a rearranged taxol derivative with tubulin assembly activity. J Org Chem 56:5114–5119.
11. Castellano EE, Hodder OJR. 1973. Crystal and molecular structure of the diterpenoid baccatin V, a naturally occurring oxetane with a taxane skeleton. Acta Crystallogr Sect B: Struct Crystallogr Cryst Chem 29:2566–2570.
12. Martin AN, Bustamante P, Chun AHC. 1993. Physical pharmacy: Physical chemical principles in the pharmaceutical sciences. Lippincott Williams & Wilkins. Philadelphia.
13. Magri NF, Kingston DGI, Jitrangsri C, Piccariello T. 1986. Modified taxols. 3. Preparation and acylation of baccatin III. J Org Chem 51:3239–3242.
14. Wiley RA, Rich DH. 1993. Peptidomimetics derived from natural products. Med Res Rev 13:327–384.
15. Vander Velde DG, Georg GI, Grunewald GL, Gunn CW, Mitscher LA. 1993. "Hydrophobic collapse" of taxol and Taxotere solution conformations in mixtures of water and organic solvent. J Am Chem Soc 115:11650–11651.
16. Williams HJ, Scott AI, Dieden RA, Swindell CS, Chirlian LE, Francl MM, Heerding JM, Krauss NE. 1993. NMR and molecular modeling study of the conformations of taxol and its side chain methyl ester in aqueous and nonaqueous solution. Tetrahedron 49:6545–6560.